Nanoscale

PAPER

View Article Online
View Journal | View Issue

Cite this: *Nanoscale*, 2025, **17**, 18377

Fusion of liposomes incorporating α-linolenic acid with the cell plasma membrane is site-restricted†

Abdullah Aljasser, ‡ Ramy Elbahr, Cynthia Bosquillon and Snow Stolnik *

This study assesses the interactions of liposomes incorporating unsaturated *cis*-9,12,15-octadecatrienoic acid (α-linolenic acid) with model and cell membranes. The liposome–cell membrane interactions that initiate a membrane fusion process may enable a direct cytoplasmic delivery of liposomal cargo. Experimental results confirm the incorporation of α-linolenic acid (αLA) into, and a consequent concentration-dependent increase in the fluidity of, the liposomal lipid bilayer, as demonstrated by ^{1}H-NMR spectroscopy and a laurdan emission assay, respectively. On mixing with simple membrane-model liposomes, Förster Resonance Energy Transfer (FRET) analysis of embedded donor–acceptor pairs reveals a reduction in the FRET ratio, indicative of structural alterations in the lipid bilayer and a membrane fusion of αLA containing liposomes, not observed for their non-αLA counterparts. Following application to cells *in vitro* a reduction in the FRET ratio was seen for both αLA-containing and non-αLA liposomes, implying changes in the liposomal lipid bilayer in both systems. However, confocal microscopy and Pearson's correlation coefficient analysis reveal a crucial difference: αLA containing liposomes preferentially localize at the cell plasma membrane, whereas their non-αLA counterparts predominantly exhibit intracellular localisation. Notably, cell membrane-associated fluorescence appears punctate and heterogeneously distributed, suggesting that αLA-liposome fusion with the cell membrane does not lead to a homogeneous mixing of lipid membrane/dye lateral diffusion but that, for the system and conditions tested, the liposome fusion is a site-restricted process. Observations in this study are critical in the design of drug delivery systems capable of achieving direct cytoplasmic delivery of active compounds to potentially overcome a current bottleneck in effective cytosolic drug delivery.

Received 7th February 2025,
Accepted 3rd July 2025

DOI: 10.1039/d5nr00560d

rsc.li/nanoscale

Introduction

Liposomes are spherical structures characterised by an arrangement of lipids into a bilayer membrane encapsulating an aqueous central space.[1,2] An extensive body of research and published literature studies investigating liposomes exist, ranging from the characterisation of their physicochemical properties,[3,4] behaviour as drug delivery systems *in vitro* and *in vivo*, to clinical studies and their current use in therapy (*e.g.* Doxil® and Caelyx®).[5] Drug targeting studies typically report that liposomes deliver therapeutic cargo *via* endocytosis by a (target) cell.[6,7] Hence, liposomes enter the cellular trafficking process that ultimately leads to a destructive lysosomal compartment, unless an incorporated functionality stimulates endosomal escape, allowing liposomes/liposomal cargo to reach cell cytoplasm.[6,8] Another option for cellular delivery considered in the field is for liposomes to fuse with the cell plasma membrane and release their cargo directly to the cell cytoplasm (cytosolic delivery).[9] The ability of nano-carriers to deliver their cargo directly to cell cytoplasm is essential to achieve the therapeutic effect of new biologics, including nucleic acids (*e.g.* RNAs), antibodies to cytosolic targets, cytosolic enzymes, or antigen presentation to the immune system.[10] The inefficient cytosolic delivery is identified as a bottleneck in the therapeutic translation of mRNA vaccine technologies.

This study investigates whether the composition of a liposomal lipid bilayer can be modified by the incorporation of the unsaturated fatty acid, α-linolenic acid (αLA), to tailor liposomal properties towards preferential cell membrane fusion and reduce their cellular internalization *via* an endocytosis pathway. The effect of the incorporation of polyunsaturated fatty acids, such as α-linolenic acid, on the fluidity of lipid bilayers has been studied previously.[11,12] Their inclusion disrupts the regular packing of phospholipid molecules in the lamellar bilayer structure, thereby enhancing the bilayer fluid-

Division of Molecular Therapeutics and Formulation, School of Pharmacy, University of Nottingham, Nottingham, NG7 2RD, UK. E-mail: snow.stolnik@nottingham.ac.uk

†Electronic supplementary information (ESI) available. See DOI: https://doi.org/10.1039/d5nr00560d

‡Current address: The Department of Pharmaceutics, College of Clinical Pharmacy, Imam Abdulrahman bin Faisal University, P.O. Box 1982, Dammam 31441, Saudi Arabia.

ity. Increased fluidity could potentially impact different membrane behaviours such as liposomal membrane fusion with the cell plasma membrane.[13]

For the composition of liposomes and simple membrane-model liposomes used in this study, the following is important to consider that model membrane fusion mediated by the poly (ethylene glycol) (PEG) presence[14] shows that even when the vesicles (liposomes) are aggregated in the presence of high concentrations of PEG, no fusion is observed between large unilamellar vesicles which are composed of a single phosphatidylcholine species.[15] PEG-mediated vesicle fusion occurs only when bilayers are somehow perturbed. Fusogenic perturbation has been shown to result from, for example, a high bilayer curvature due to acyl chain unsaturation present within small, unilamellar vesicles (as used in this study), the presence of a small fraction of certain amphipaths, and imperfect outer leaflet lipid packing. Both apposing membranes must be perturbed in their outer leaflets, and fusion does not occur when perturbation is absent/blocked.[16,17] The literature thus emphasizes the importance of imperfect lipid packing in the membrane leaflets which are in contact with each other as the condition necessary to drive the lipid rearrangements needed to initiate bilayer fusion.

The fusion of liposomes with the cell plasma membrane is often investigated employing Förster Resonance Energy Transfer (FRET). Cyanine-based fluorescent probes have typically been used as FRET donor–acceptor pairs in liposomal systems as they possess the molecular structure and lipophilicity (aliphatic chain and log $P > 10$) that drives their incorporation within the lipophilic environment of the liposomal lipid bilayer.[18,19] For example, a FRET pair of the DiO donor and DiI acceptor (as adopted in this study) was used to assess the phosphatidylcholine (PC) liposome–cell membrane fusion with a range of different cells in culture;[18] a membrane fusion between liposomes incorporating the NK cell membrane and MCF-7 cells was assessed by separately loading BHK21 cells with the donor (CF350) and the liposomes with the acceptor (NBD) probe. The successful membrane fusion was confirmed by an increase in the FRET efficiency (inter-FRET approach).[20]

Here we investigate interactions between liposomes and model membranes and cells in *in vitro* culture as a function of α-linolenic acid (αLA), *i.e.* acyl chain unsaturation content in the liposomes. The DiO and DiI FRET pair was incorporated into the liposomal lipid bilayer to evaluate membrane fusion applying both fluorescence spectroscopy and flow cytometry analyses. Confocal microscopy with Pearson coefficient analysis was employed to obtain critical spatial information on αLA-liposome interactions with the cells in the culture.

Experimental

Materials

1,2-Distearoyl-*sn-glycero*-3-phosphocholine (DSPC), 1,2-dioleoyl-*sn-glycero*-3-phosphoethanolamine (DOPE), *N*-(dodecanoyl)-sphing-4-enine-1-phosphocholine (sphingomyelin), and cholesterol were purchased from Avanti® Polar Lipids, Inc. (UK). 1,2-Dioleoyl-*sn-glycero*-3-phosphocholine (DOPC) was obtained from NOF Corporation, COATSOME® MC-8181 (Japan). *cis*-9,12,15-Octadecatrienoic acid (α-linolenic acid) was purchased from Thermo Fisher® Chemicals (USA). DiO (3′-dioctadecyloxacarbocyanine ($DiOC_{18}$ (3))), DiI (1,1′-dioctadecyl-3,3,3′,3′-tetramethylindocarbocyanine ($DiIC_{18}$ (3))), 5(6)-carboxyfluorescein, plasma membrane CellMask™, and DAPI were supplied by Sigma Aldrich (UK).

Methods

Preparation of liposomes

Liposomes were fabricated by the classical thin film hydration method.[21] The lipids were dissolved in chloroform (1 mg ml^{-1}) and the required volumes of solutions were mixed to obtain the liposome compositions specified in Table 1. To produce fluorescent liposomes, 20 μl of DiO, DiI, or both (dissolved in $CHCl_3$) were added during the preparation of the lipid mixture in the organic solvent. The organic solvent was evaporated under nitrogen stream to form a thin film on the wall of a rotating flask. The films were hydrated with filtered (0.2 μm) phosphate-buffered saline (PBS) (10 mM at pH 7.4). After the hydration step, all initial liposome formulations were extruded 11 times through a 200 nm filter membrane using an Avanti Polar Lipids, Inc. extruder. A PD-10 desalting column (Cytiva) was used to remove unincorporated dyes according to the manufacturer's protocol.

Particle size and zeta potential analyses

The hydrodynamic particle diameter and zeta potential of fabricated liposomes were measured using a Zetasizer Nano (Malvern). Prior to each measurement, samples were appropriately diluted with 10 mM PBS buffer (pH 7.4). Results are presented as the mean ± standard deviation of three repeated measurements. Particle size distribution profiles are shown in ESI Fig. S1.†

Table 1 Summary of liposome compositions

	mol%					
Liposomes	DOPC	DSPC	Chol	SM	DOPE	αLA
Simple membrane model	50.0	27.0	23.0			
$αLA_0$-DiO&DiI [a]		62.5	25.0	6.25	6.25	0
$αLA_0$-DiO		62.5	25.0	6.25	6.25	0
$αLA_0$-DiI		62.5	25.0	6.25	6.25	0
$αLA_{10}$-DiO&DiI		56.3	22.5	5.6	5.6	10
$αLA_{20}$-DiO&DiI		50.0	20.0	5.0	5.0	20
$αLA_{20}$-DiO		50.0	20.0	5.0	5.0	20
$αLA_{20}$-DiI		50.0	20.0	5.0	5.0	20
$αLA_{30}$-DiO&DiI		43.7	17.5	4.4	4.4	30
$αLA_{40}$-DiO&DiI		37.5	15.0	3.75	3.75	40

[a]All DiO&DiI-liposomes contain 20 μM DiO and DiI dyes. $αLA_0$-DiO and $αLA_{20}$-DiO liposomes contain 20 μM DiO. $αLA_0$-DiI and $αLA_{20}$-DiI contain 20 μM DiI.

Quantification of α-linolenic acid incorporation

To analyse the αLA content in liposomes, 300 μl of the extruded liposome suspension was freeze-dried and the resulting powder reconstituted in 750 μl of $CDCl_3$, and 50 μl of a 10 mg ml^{-1} solution of benzoic acid (BA) in $CDCl_3$ was added as a reference standard. The ^1H Nuclear Magnetic Resonance (NMR) spectra of the samples were acquired using a Bruker 400 MHz NMR spectrometer. The α-linolenic acid peak, identified at 2.8 ppm and representing 4 protons, and the benzoic acid peak at 7.6 ppm, representing 1 proton, were analysed using MestReNova software. The α-linolenic acid concentration in the analysed sample was calculated from the following equation:

$$\alpha\text{LA conc} = \frac{\int \alpha\text{LA}}{\int \text{BA}} \times \frac{\text{no. of proton BA}}{\text{no. of proton } \alpha\text{LA}} \times \text{conc. of BA.}$$

The efficiency of linolenic acid incorporation into liposomes was calculated from:

$$\alpha\text{LA incorporation efficiency, \%} = \frac{\alpha\text{LA conc. after column}}{\text{initial } \alpha\text{LA conc.}} \times 100$$

whereby αLA concentration after column separation was calculated from αLA concentration in liposome samples determined by ^1H-NMR, while initial αLA concentration arises from the amount of αLA added to the formulation.

Membrane fluidity measurements

To assess the effect of αLA on the membrane fluidity of liposomes, general polarization of laurdan was determined. The laurdan probe was added to the organic solvent stage during liposome production. The stock solution of laurdan used was 1 mg ml^{-1} in $CHCl_3$ and the concentration of laurdan in the liposomes, relative to the total molar lipid concentration, was 0.2 mol%. Liposomes were then fabricated as described above. Laurdan containing liposome suspensions were diluted to 1 : 5 with 10 mM PBS buffer at pH 7.4, and 100 μl samples were placed in three black bottom 96-well plates. These were incubated at 4, 25, or 37 °C for 1 h. Fluorescence measurements for each plate were recorded at a relevant temperature using a Tecan infinite 200 PRO multimode plate reader. Fluorescence intensities were recorded at λ_{em} 440 (I_{440}) and 490 (I_{490}) nm after excitation at λ_{ex} 360 nm and used to calculate the generalized polarization (GP) using the following equation:

$$\text{GP} = \frac{I_{440} - I_{490}}{I_{440} + I_{490}}.$$

Incorporation of fluorescent dyes into liposomes

After the fabrication of the liposomes, the liposome suspensions were diluted to 2.5 ml of the total volume and run on a PD-10 desalting column (Cytiva) eluted with 10 mM PBS, at pH 7.4, as per the manufacturer's protocol. Fluorescence of the eluted fraction was read (Tecan Infinite 200 PRO multimode plate reader) at λ_{ex} 460 nm and λ_{em} 505 or 565 nm. The incorporation efficiency was calculated from fluorescence intensities before and after elution. The dye incorporation data are shown in ESI Fig. S2.†

Incorporation of FRET pair probes

To confirm the incorporation of FRET pair dyes into liposomes, an 80 μl sample was taken from a liposome formulation following chromatographic separation, placed into a black bottom 96-well plate and 20 μl of either DMF or THF was added. Fluorescence of the liposome suspensions either in the absence or in the presence of an organic solvent was recorded at λ_{ex} 460 nm and λ_{em} 495 to 650 nm (Tecan Infinite 200 PRO multimode plate reader). The FRET ratio was calculated based on the following equation:

$$\text{FRET ratio} = \frac{I_{\text{DiI}}}{I_{\text{DiO}} + I_{\text{DiI}}}$$

where I_{DiO} and I_{DiI} are the fluorescence intensities of DiO at λ_{em} 505 nm and DiI at λ_{em} 565 nm. Data are shown in ESI Fig. S3.†

Evaluation of liposome permeability using carboxyfluorescein

Liposomes were formulated as described above, with one modification in the hydration step. The lipid film was hydrated with filtered PBS buffer containing 40 mM carboxyfluorescein. Free (unencapsulated in liposomes) carboxyfluorescein was removed using a PD-10 column. To dissolve carboxyfluorescein at this high concentration NaOH was added to bring the pH to 7.4–7.6. CF is self-quenched at high concentration inside the liposomes and fluoresces once it leaks out of liposomes. CF-containing liposomes were diluted to 1 : 5 with PBS or 0.2% Triton-X 100. The 100 μl samples were placed in a black bottom 96-well plate (4 plates in total). The first plate was read at time 0 h and 25 °C. The three plates were incubated for 2 h at different temperatures, 4, 25, and 37 °C. The fluorescence was read (Tecan Infinite 200 PRO multimode plate reader) at λ_{ex} = 485 nm and λ_{em} = 520 nm. The release of CF from the liposomes was calculated as:

$$\%\,\text{CF release} = \frac{F_{\text{CF}}^{t} - F_{\text{CF}}^{t=0}}{F_{\text{CF}}^{\infty} - F_{\text{CF}}^{t=0}}$$

where F_{CF}^{t} = fluorescence intensity of CF liposomes at time t, $F_{\text{CF}}^{t=0}$ = fluorescence intensity of CF liposomes at time 0 and $F_{\text{CF}}^{t=\infty}$ = fluorescence intensity of CF liposomes after lysing 0.2% Triton-X 100.

Liposome mixing

The suspension of simple membrane model liposomes (Table 1) was mixed with FRET pair containing liposomes with an increased content of α-linolenic acid, *i.e.* αLA_0-, αLA_{10}-, αLA_{20}-, αLA_{30}- and αLA_{40}-DiO&DiI liposomes, in a 1 : 1 v/v ratio and incubated overnight in a water bath at 37 °C with continuous gentle shaking at 150 rpm. Fluorescence of the suspension mixture was measured at λ_{ex} 460 nm with the emission spectrum being collected from λ_{em} 490 to 650 nm. FRET ratios were calculated from the fluorescence intensity scans of the

suspension mixtures recorded before and after water bath incubation (at 0 h and 24 h),

$$\text{FRET ratio} = \frac{I_{\text{DiI}}}{I_{\text{DiO}} + I_{\text{DiI}}}$$

where I_{DiO} and I_{DiI} are the fluorescence intensities of DiO at λ_{em} = 505 nm and DiI at λ_{em} = 565 nm.

Cryogenic transmission electron microscopy (Cryo-TEM)

αLA_{20}-DiO&DiI liposomes were mixed with simple model membrane liposomes (Table 1) in a 1 : 1 v/v ratio and incubated for 10 minutes. The samples were then prepared using a Gatan CP3 cryo-plunge and imaged on a JEOL 2100+ TEM operating at 200 kV. The sample (3 μL) was deposited onto a holey carbon copper TEM support grid, that had been glow discharged to induce hydrophilicity, in a controlled humidity and temperature environment (25 °C, 80% humidity), and blotted on both sides of the TEM grid (1.5 s), before gravity plunging into liquid ethane (−172 °C) to vitrify. The samples were maintained under liquid nitrogen (−196 °C) during transfer to a TEM cryo-sample holder (Gatan 926), and the temperature was held at around −176 °C throughout imaging using a Gatan (Smartset model 900) cold stage controller. Images were recorded (Gatan Ultrascan 100XP camera), with a nominal under a focus value of 3–5 μm and a 60 μm objective aperture to enhance the phase contrast.

Liposome cell toxicity

Human lung epithelial adenocarcinoma A549 cells were obtained from the American Type Culture Collection (ATCC, CCL-185). The cells were cultured in 75 cm^2 flasks until 80–90% confluency in DMEM medium (10% FBS, and 1% penicillin/streptomycin) prior to any further experiment. Liposome toxicity was assessed by the metabolic activity MTS assay following a standard protocol. Cells were seeded at a density of 1×10^4 cells in a 96-well plate in DMEM medium (10% FBS, and 1% penicillin/streptomycin). The plates were incubated for 24 h before the medium was aspirated and the cells were washed with pre-warmed 10 mM PBS (pH 7.4). Tested liposomes (αLA_0-DiO&DiI and αLA_{20}-DiO&DiI) were added and the cells were exposed for 24 h. The cells were then incubated with MTS reagent for 3 h. For positive and negative control, the cells were incubated either with 1% v/v Triton-X solution or DMEM medium, respectively. The absorbance was recorded at 490 nm (Tecan Infinite 200 PRO multimode plate reader). The cell viability was calculated as below, where X corresponds to the absorbance of liposome treated cells. Data are shown in ESI Fig. S4.† Further experiments were hence conducted using αLA_0- and αLA_{20}-DiO&DiI liposomes at total lipid concentrations below 1 mM.

$$\text{Cell viability} = \frac{X - \text{positive control}}{\text{negative control} - \text{positive control}} \times 100$$

Liposome interaction with cells assessed by fluorescence spectrophotometry

A549 cells were seeded in 24-well plates at a density of 5×10^4 and incubated until 80% confluency prior to incubation with the tested formulations. The cells were incubated for 4 hours (5% CO_2, 37 °C, and with 95% relative humidity) with αLA_0-DiO, αLA_0-DiI, and αLA_0-DiO&DiI liposomes and αLA_{20}-DiO, αLA_{20}-DiI, and αLA_{20}-DiO&DiI liposomes. The cells were then washed twice with 10 mM PBS (pH 7.4). The cells were fixed with 4% PFA for 10–15 minutes. The fixed cells were washed twice with 10 mM PBS (pH 7.4) and incubated with 300 μl of 10 mM PBS (pH 7.4). Liposome association with cells was assessed by reading the fluorescence (Tecan Infinite 200 PRO multimode plate reader) at λ_{ex} = 460 nm and λ_{em} = 505 or 565 nm. FRET ratios were calculated as described in specific experiments and relevant figures.

Liposome interaction with cells assessed by flow cytometry

A549 cells were seeded in a 24-well plate at a density of 5×10^4 and incubated until 80% confluency prior to their incubation with the tested formulations. The cells were exposed for 4 h (5% CO_2, 37 °C, and with 95% relative humidity) to the tested liposomes: αLA_0-DiO, αLA_0-DiI, αLA_0-DiO&DiI and αLA_{20}-DiO, αLA_{20}-DiI, and αLA_{20}-DiO&DiI liposomes. The tested samples were removed, the cells were washed twice with prewarmed 10 mM PBS (pH 7.4), and then detached using 300 μl of 2.5% trypsin–EDTA. The suspensions were diluted with 300 μl of fresh medium to inactivate trypsin. These suspensions were centrifuged at 1200 rpm for 5 minutes. The pellets were fixed with 200 μl of 4% v/v paraformaldehyde (PFA) for 10–15 min and then diluted with 300 μl of 10 mM PBS (pH 7.4). Cellular association of the liposomes was assessed using a SONY ID7000 flow cytometer and analysed using Kaluza Analysis Software. The FRET ratio was calculated as a ratio of the fluorescence intensity values of DiO emission in DiO-liposomes (I_{D}) relative to DiO emission fluorescence from DiO&DiI-liposomes (I_{DA}) upon excitation at λ_{em} 488 nm using the following equation:

$$\text{FRET ratio} = 1 - \frac{I_{\text{DA}}}{I_{\text{D}}}.$$

Liposome interaction with cells assessed by confocal laser scanning microscopy

To acquire fluorescence images by confocal laser scanning microscopy (CLSM), Nunc™ Lab-Tek™ II Chambered Coverglass 8 wells were used. The cells were seeded at a density of 5×10^4 and incubated until 80% confluency prior to the incubation with the tested formulations. The cells were incubated for 4 h (5% CO_2, 37 °C, and with 95% relative humidity) with αLA_0-DiO, αLA_0-DiI, and αLA_0-DiO&DiI liposomes and αLA_{20}-DiO, αLA_{20}-DiI, and αLA_{20}-DiO&DiI liposomes. The cells were then washed once with 10 mM PBS (pH 7.4), and the plasma membrane was stained by the addition of Deep red CellMask™ before the cells were fixed with 4% v/v PFA. The cells were then washed once with 10 mM PBS (pH

7.4), and the nuclei were stained with DAPI. The images were collected using Leica TCS SPE high-resolution spectral confocal microscopy. All images were analysed using Fiji image J analysis software by only adjusting the brightness and contrast. For the co-localization, the Jacob plugin was used between the fluorescent liposomes applied on the cells and the plasma membrane staining. This statistical analysis is used to quantify the similarity, or correlation between the pixel intensity of two 'colours'.[22]

Statistical analysis

Data are normally presented as the mean ± standard deviation (SD), or ± standard error of mean (SEM) from three or four replicates. Analysis of variance (ANOVA) test with Tukey's multiple comparisons of means between groups was typically employed; a P value of <0.05 was considered statistically significant. The notations used in the presentation of statistical significance: ****, ***, **, and * correspond to p-values of $p < 0.0001$, $p < 0.001$, $p < 0.01$, and $p < 0.05$, respectively.

Results and discussion

Composition and physicochemical characterization of liposomes

Considering lipid compositions of liposomes used in this study, α-linolenic acid (α-LA) was incorporated into liposomes comprising DSPC, cholesterol and DOPE (Table 1), the lipid components typically used in liposomes and lipid nanoparticles intended for drug delivery.[23] Addition of cholesterol would be expected to increase the packing of lipid molecules in a lamellar bilayer, while added sphingomyelin would be expected to, with cholesterol, form phase separated sphingomyelin-cholesterol rich domains ('raft').[24] Regarding membrane fusion, it has been proposed that phase-separated domains containing cholesterol mediate close approach of the apposing membranes, whereby molecular packing defects at the domain boundaries mediate hydrophobic interaction and membrane fusion.[16,25] DOPE is demonstrated to promote the formation of a negative curvature in the bilayer structure, with the presence of DOPE and cholesterol facilitating membrane fusion through an increase of curvature stress, the promotion of the highly curved inverted hexagonal phase (H_{II}), and the reduction of the energy required to dehydrate the membrane and facilitate a close bilayer contact.[26]

Fig. 1 summarizes the physicochemical properties of αLA-liposomes. The data show liposomes with an average diameter in the sub-200 nm size range, with a relatively narrow particle size distribution (polydispersity index < 0.2). This particle size is typically used in the design of delivery systems for intracellular drug delivery and is amenable for cellular internalisation *via* endocytosis – important for this work in the view of a 'control' system undergoing endocytosis.[27] Particle size decreases with the incorporation of α-linolenic acid, compared to αLA_0-liposomes; a reduction from 182 ± 6.7 nm for 0 mol% αLA in αLA_0-DiO&DiI to 146 ± 3.3 nm for 40 mol% αLA containing αLA_{40}-DiO&DiI liposomes. This decrease is statistically significant and indicates the effect of αLA on the lipid bilayer assembly and behaviour.

It should be noted that intensity, number, and volume particle size distribution profiles (ESI, Fig. S1†) indicate the absence of species in a size range of around 10 nm which, if present, would indicate the existence of assemblies (micelles) that could form from α-linolenic acid molecules present in an aqueous medium.[28] This also suggests that the incorporation of α-linolenic acid into liposomes has occurred.

Fig. 1 further shows that the modulus of the negative zeta potential gradually increases from −4.6 ± 1.9 mV for αLA_0-

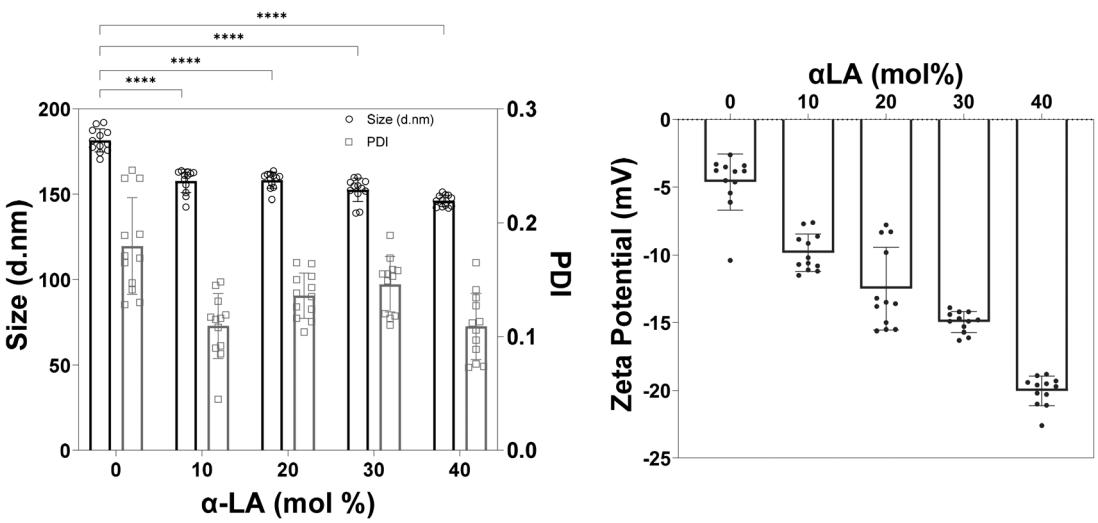

Fig. 1 Liposomes' average hydrodynamic particle diameter and polydispersity index (PDI), and zeta potential. The data for αLA-DiO&DiI liposomes containing different mol% of αLA ranging from 0 to 40 mol% are presented. The measurements were on three replicate formulations (N = 3), and each replicate was measured four times (n = 4), average ± SEM. Statistical analysis 2-way ANOVA with Tukey's multiple comparison test.

DiO&DiI (0 mol% of αLA) on the addition of increasing mol% of α-linolenic acid, reaching −20.3 ± 1 mV for αLA_{40}-DiO&DiI liposomes, measured in 10 mM PBS buffer (pH 7.4). The trend can be ascribed to deprotonation of the carboxylic acid group of α-linolenic acid in pH 7.4 buffer, pointing again to the α-linolenic acid incorporation into the liposomes' lipid bilayer. In general, zeta potential values are relatively low (Fig. 1), and below values are usually considered necessary to provide electrostatic stabilization of a colloidal dispersion. Colloidal stability of the liposomes, as indicated by narrow particle size distribution and low polydispersity index (Fig. 1 and ESI Fig. S1†), could be attributed to the 'hydration force' of surface adsorbed hydrated ions from the dispersion medium used[29] and contribution of the residual charge ('smeared charge') of the zwitterionic heads of phospholipids.[30–32]

In the context of the current study, it is important to notice that variations in the surface charge (zeta potential), as well as the nature of this charge, have been shown to significantly influence liposome interactions with, and internalisation by cells in the culture.[6,33] For example, mechanisms of internalisation for zwitterionic (DOPC) and negatively charged (DOPG) liposomes in HeLa cells were found to be mediated by different endocytosis pathways.[34] Here the incorporation of increasing levels of α-LA creates liposomes with increasingly negative surface charge (Fig. 1), which could influence their interactions with lipid bilayer membranes and should be considered during the data interpretation. Regarding liposome–cell membrane fusion, previous research reported that negatively charged liposomes, particularly those containing phosphatidylserine (PS), can induce significant fusion with the cell membrane, whilst liposomes containing phosphatidylcholine (PC) do not typically induce such fusion.[9]

Quantification of αLA incorporation into liposomes by ^{1}H NMR

The ^{1}H NMR spectrum (Fig. 2) shows a characteristic peak of α-linolenic acid at 2.78 ppm,[35] with a triplet indicating that the protons responsible for this peak are surrounded by two neighbouring protons. There are 4 such protons in α-linolenic acid (highlighted in red in Fig. 2). As an internal standard, benzoic acid was added in a known amount to the liposome samples. The peaks of benzoic acid are evident in the spectrum, and the proton peak at 7.6 ppm (highlighted in red in Fig. 2) was used for calculations, as described in the Methods section.[35] The

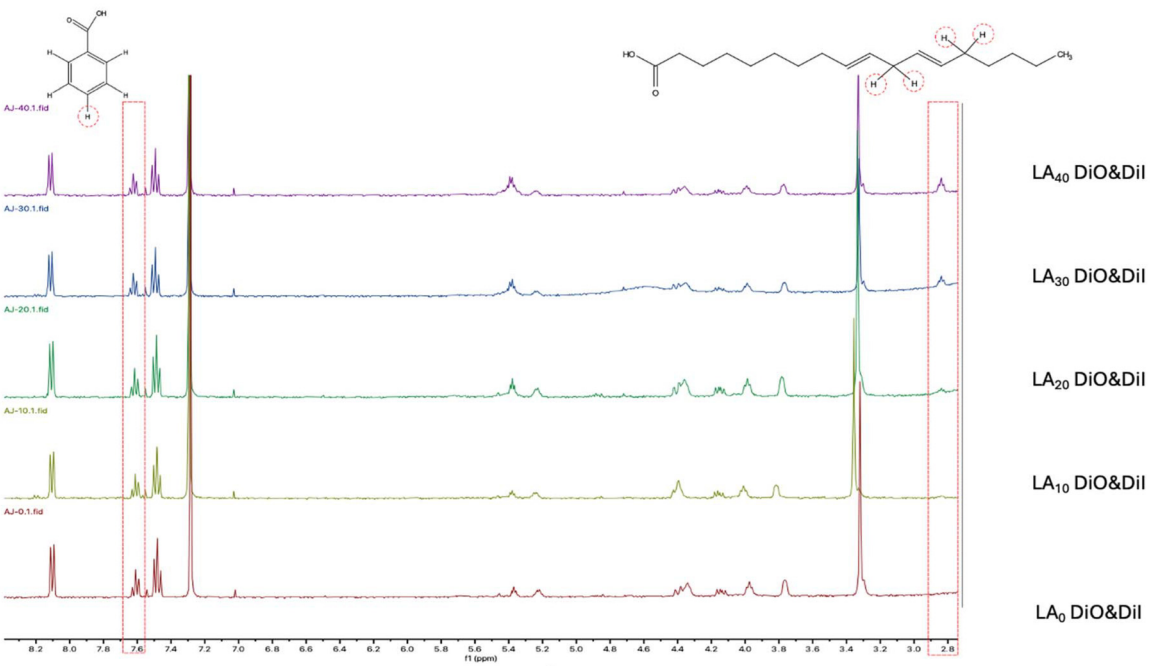

Liposomes	LA_{10}DiO&DiI	LA_{20}DiO&Di	LA_{30}DiO&Di	LA_{40}DiO&DiI
LA- incorporation efficacy	54.6 ± 1	93.7 ± 2	100.8 ± 2	77.2 ± 4

Fig. 2 Quantification of α-linolenic acid in liposomes using ^{1}H NMR spectroscopy. ^{1}H NMR spectra of DiO&DiI-liposomes containing different molar percentages of α-linolenic acid (αLA) ranging from 0 to 40 mol%. The liposomes were freeze dried and dissolved in $CDCl_3$ and 0.5 mg benzoic acid (BA) added as a reference standard. The α-linolenic acid and benzoic acid integrated peaks were used for the quantification. The red boxes represent the protons of αLA and BA. Content of α-linolenic acid, and incorporation efficacy into liposomes shown in the table is expressed as percentages of the α-LA content compared to the original concentrations added during liposomes preparation. The experiment was performed with three replicates (N = 3).

data show that the incorporation efficacy of α-linolenic acid in the liposomes was relatively high (Fig. 2, table). The experimentally determined molar ratio of αLA in liposomes is hence, in general, in line with the input, apart from αLA_{10}-liposomes; for simplicity, we hence refer to liposomes using their input αLA content.

The effect of incorporation of α-linolenic acid on the fluidity of the liposomal membrane

The effect of α-linolenic acid (αLA) incorporation on the membrane fluidity of liposomes was assessed using a classical laurdan generalized polarization analysis.[36,37] The results, presented in Fig. 3, reveal a decrease in the generalized polarization (GP) values of laurdan as the content of αLA in liposomes increases, relative to liposomes containing no αLA. GP values are indicative of the lipid bilayer's structural order, whereby the higher the value the more ordered the structure.[38] The data hence indicate that there is an increase in the lipid bilayer fluidity as the content of αLA in liposomes is increased. A looser packing due to the incorporation into the lipid bilayer of lipids with unsaturated acyl chain (linolenic acid contains 3 *cis* double bonds, Fig. 2) has been reported to lead to a disordered membrane structure and promotion of hexagonal phase packing of the liquid crystalline phase.[39] In turn, fusion efficiency between membranes was shown to depend on membrane fluidity parameters, such as membrane viscosity and bending rigidity.[39] For instance, recent molecular dynamics simulations revealed that the inner leaflet of the plasma membrane is more fusogenic than the outer one due to the high fraction of unsaturated lipids and high fluidity.[40]

The data (Fig. 3) further indicate a significant increase in the bilayer fluidity with an increase in temperature, in agreement with previous studies.[2,41,42] One should note a highly significant increase in the membrane fluidity (decrease in GP) for liposomes at 37 °C, the temperature at which membrane fusion studies were conducted both with a simple membrane-model system and cells in culture.

To assess the balance in liposome membrane fluidity, potentially resulting in an increase in membrane permeability, and their ability to carry incorporated cargo, carboxyfluorescein (CF) assay, accepted in the field as a routine method for assessing membrane permeability, was conducted (Fig. 3). In general, the profiles show relatively low levels of CF leakage from liposomes, below 10% in a 2-hour experiment. The CF release increases with an increase in the αLA content and the incubation temperature, as it would be expected from laurdan generalized polarization data (Fig. 2) and was previously reported.[43] The data hence indicate the ability of the designed liposomes to incorporate and retain, for a period of time, a water-soluble cargo.

The effect of α-linolenic acid on membrane fusion

In this experiment, α-linolenic acid-containing liposomes, which incorporate DiO and DiI FRET pair probes, *i.e.* αLA_0-, αLA_{10}-, αLA_{20}-, αLA_{30}-, and αLA_{40}-DiO&DiI liposomes, were incubated with simple membrane-model liposomes (Table 1 and ESI Fig. S1†) at 37 °C. The composition of simple membrane-model liposomes (DOPC, DSPC and cholesterol) was selected, as previous studies of this three-component system demonstrate complex phase behaviour and phase co-existence. DOPC shows unfavourable interactions with cholesterol and DSPC, which results in macroscopic liquid/liquid separation in various compositions.[22,44,45] Mixtures of cholesterol with one phospholipid with a relatively high melting temperature

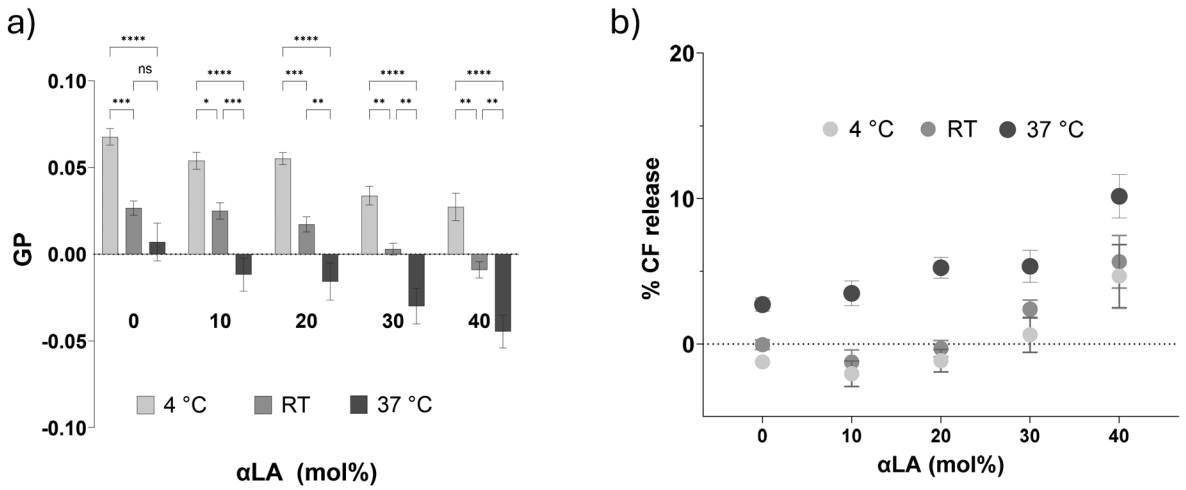

Fig. 3 (a) Laurdan generalized polarization (GP) of liposomes with different α-linolenic acid (αLA) content measured at three different temperatures. Fluorescence of αLA_0-, αLA_{10}-, αLA_{20}-, αLA_{30}-, and αLA_{40}-DiO&DiI liposomes measured after 1 h of incubation at 4 °C, room temperature (RT–20 °C), and 37 °C at λ_{em} 440 nm and λ_{em} 490 nm after excitation λ_{ex} 360 nm. GP calculated from intensities I_{440} and I_{490}. The experiment was performed with four formulation replicates (N = 4), and each replicate was measured three times (n = 3) ± SEM. (b) The effect of αLA content on the permeability of liposomes to carboxyfluorescein (CF). The CF release (%) was measured at a 2 h time point at different temperatures. The experiment was performed with three replicates (N = 3), and each replicate was measured five times (n = 5), average ± SEM. Statistical analysis 2-way ANOVA with Tukey's multiple comparison test.

(DSPC) together with another phospholipid with a relatively low melting temperature (DOPC) are viewed as useful models for the outer leaflet of cell plasma membranes, as they contain a representative compound from each of the three major membrane constituent groups.[44]

Fig. 4 summarizes calculated FRET ratios for the tested systems. For αLA_0-DiO&DiI liposomes (containing no αLA), the FRET value is high (0.86 ± 0.02) and it does not appreciably change following incubation with simple membrane-model liposomes for 24 hours at 37 °C. For αLA-containing liposomes, αLA_{10}-, αLA_{20}-, αLA_{30}- and αLA_{40}-DiO&DiI-liposomes, the data reveal a more complex picture. Here, a significant decrease in FRET values is seen even before the incubation of αLA-liposomes with simple membrane-model liposomes (Fig. 4a), apart from low αLA content liposomes, αLA_{10}. There is no significant further decrease in FRET ratios after the 24-hours incubation at 37 °C. For high αLA content αLA_{40}-liposomes the FRET values might even appear somewhat increased on mixing with simple membrane-model liposomes, although this is not statistically significant. The observed absence of a significant change in the FRET ratio after liposome mixing would suggest that membrane fusion between the αLA-containing liposomes and simple membrane-model liposomes has not occurred. In contrast, cryo-TEM images (Fig. 5) indicate the presence of membrane 'docking' and liposomal membrane 'unions' which are consistent with the cryo-TEM images in the literature, in terms of morphological appearance of liposomal membrane fusion.[46,47] Namely, the images for mixture of αLA_{20}-containing and simple membrane-model liposomes show examples of extensive membrane contact zones what is potentially an intermediate state of vesicle fusion in which the deformation of round liposomes would be separated by a single bilayer. This observation would agree with the

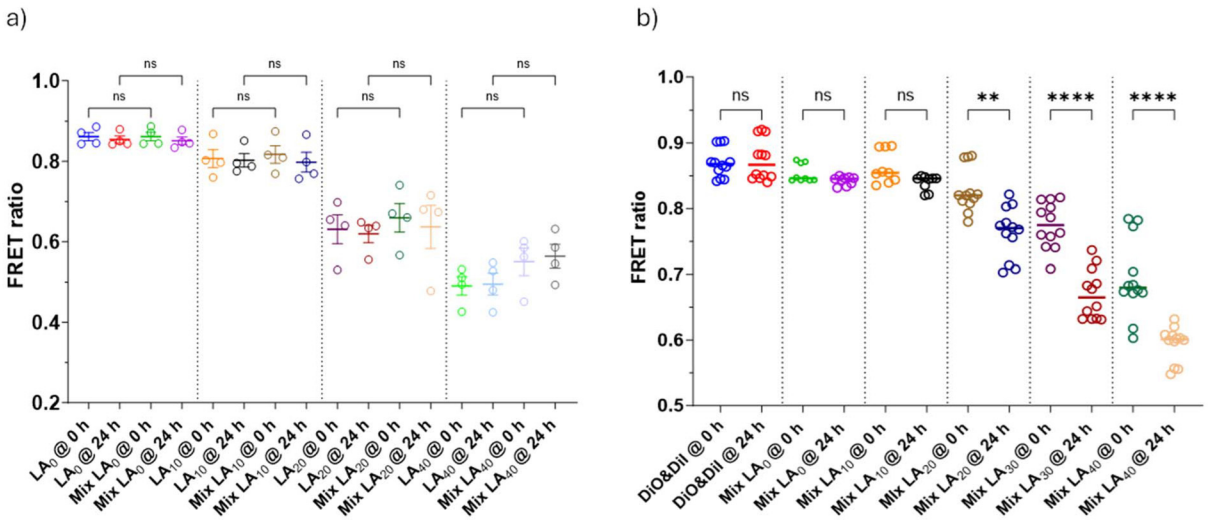

Fig. 4 FRET ratios of liposome systems before and after mixing. (a) αLA-DiO&DiI-liposomes mixed with non-fluorescent liposomes (simple DSC liposomes, table). αLA-DiO&DiI-liposomes with different mol% of αLA ranging from 0–40 mol% were used. (b) FRET ratios of DiO&DiI-liposomes following mixing with α-LA containing liposomes. αLA-liposomes with different mol% of αLA ranging from 0–40 mol% were used. For (a) and (b) the fluorescence was measured immediately following mixing, at approximately 10 minutes (denoted as '@0 h') and after 24 hours (@24 h) incubation at 37 °C with. The FRET ratios were calculated from: $I_{DiI}/(I_{DiO} + I_{DiI})$ where I_{DiO} and I_{DiI} are the fluorescence emission intensities of DiO at λ_{em} = 505 nm and DiI at λ_{em} = 565 nm. The experiment was performed with four replicates (N = 4), and each replicate was measured three times (n = 3); average ± SEM; statistical analysis 2-way ANOVA.

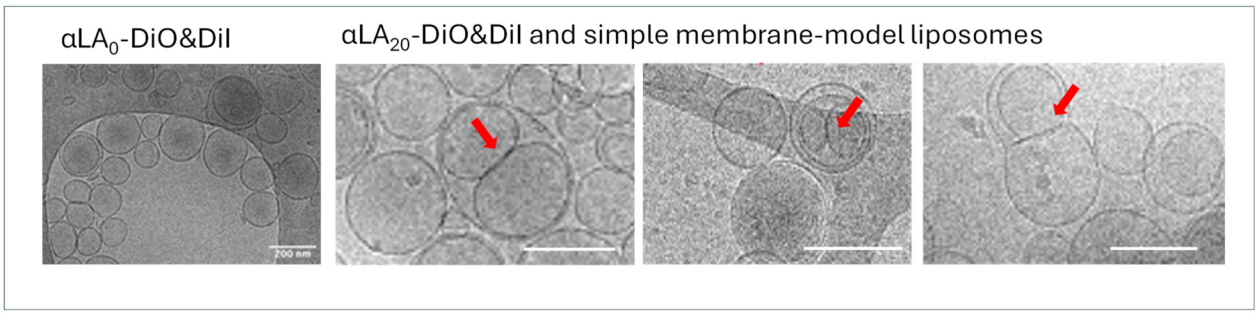

Fig. 5 Cryo-TEM images for the mixing of αLA_{20}-DiO&DiI liposomes and simple membrane-model liposomes (scale bar 200 nm). Red arrows point out the membrane fusion events. The sample of liposome containing no αLA (αLA_0 DiO&DiI) is also shown.

lipid-stalk model within the hemi-fusion pathway, which includes a diaphragm formed between the inner leaflets of the two membranes.

The observed reduction in FRET on increased αLA content in the liposomal bilayer may possibly be ascribed to the effect of α-linolenic acid on increasing liposomal membrane fluidity, as evident from the laurdan GP experiment (Fig. 3). Namely, it has been reported that FRET is affected by the orientational freedom of the donor and acceptor probes incorporated within the lipid bilayer membranes, the membrane composition, and phase sep-

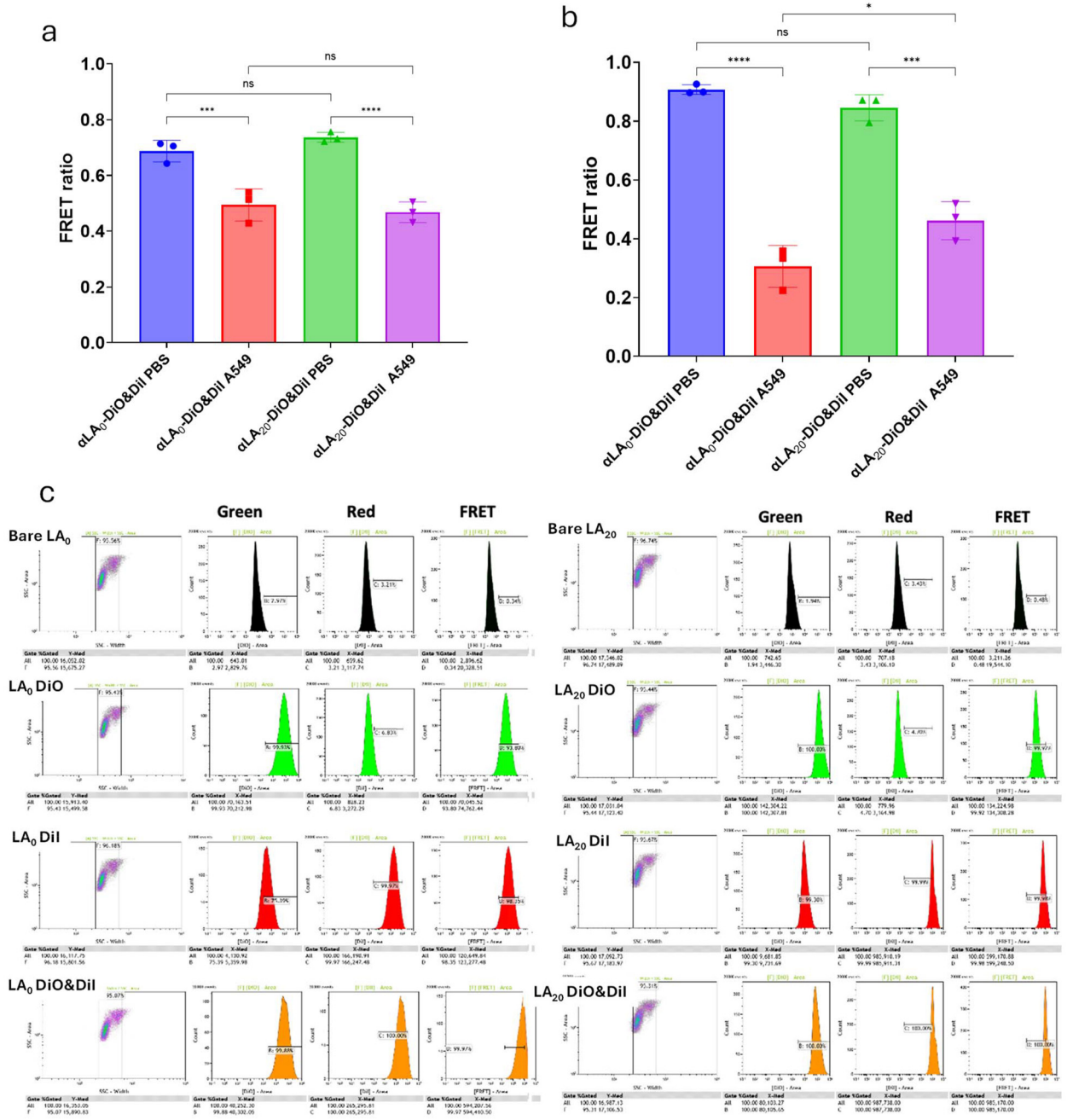

Fig. 6 Calculated FRET ratios for αLA_0-DiO&DiI and αLA_{20}-DiO&DiI liposomes in graphs (a) and (b). FRET ratios were calculated as the ratio of the fluorescence intensity values of DiO emission in DiO-liposomes relative to DiO fluorescence emission from DiO&DiI-liposomes as: $1 - (I_{DA}/I_D)$, where I_{DA} and I_D are fluorescence intensity of DiO in the DiO-liposome and in DiO-DiI liposomes. (a) FRET ratios calculated from fluorescence spectrophotometry measurements of DiO donor emission at λ_{em} 505 nm upon excitation at λ_{ex} 460 nm. (b) FRET ratios calculated from the flow cytometry analysis; donor excitation at λ_{ex} 488 nm and emission reading using filter at λ_{em} 506–554 nm. The experiment was performed with three replicates (N = 3), and each replicate was measured three times (n = 3), average ± SEM. Statistical analysis one-way ANOVA. (c) Histogram plots of the flow cytometry analysis of liposomes applied to the A549 cell line for 4 h at 37 °C. The samples were measured at green DiO (λ_{ex} = 488 nm and λ_{em} = 506–554 nm), red DiI (λ_{ex} = 561 nm and λ_{em} = 566–590 nm), and FRET (λ_{ex} = 488 nm and λ_{em} = 566–590 nm) channels.

aration within the membrane.[48] For instance, for coumarin dyes (as used here) the efficiency of energy transfer between the donor and acceptor was found to be dependent on the membrane fluidity, which authors experimentally changed by temperature changes.[49] The effect was more significant in the case of the C-153-Rh6G pair than the C-151-Rh6G pair, and attributed to different locations of the dyes inside the lipid bilayer. It is beyond the scope of this study, but further experiments, as conducted by Ghatak *et al.*,[49] would be required to understand the effect that αLA incorporation into lipid bilayer has on the DiO and DiI FRET probes interplay and behaviour. Furthermore, one would need to consider a complex interplay between the membrane composition and the preference for probe incorporation.[50] For instance, DiO was reported to incorporate more efficiently into liquid disordered phases (as present in αLA-liposomes) compared to gel phases.[50]

The 'opposite' experiment was hence designed where non-DiO&DiI-αLA$_{10–40}$-liposomes (liposomes that contain different mol% of αLA, but no FRET pair DiO and DiI) were mixed with DiO&DiI-simple membrane-model liposomes (FRET dyes containing simple membrane-model liposomes that do not contain αLA). This experiment (Fig. 4b) shows a statistically significant decrease in FRET ratios following mixing for αLA$_{20–40}$ liposomes with simple membrane-model liposomes, clearly indicating that the fusions between liposomal membranes occurred, an event that was absent for liposomes without αLA. The increased propensity for membrane fusion with an increase in the local membrane disorder,[25] could explain the observed difference in the membrane fusion of αLA$_{20–40}$ liposomes, that possess higher membrane fluidity/disorder, relative to the lack of membrane fusion for liposomes without αLA.

Assessment of liposome interactions with cells in culture

αLA$_{20}$ – liposomes were used to assess interactions with cells in *in vitro* cell culture, however to follow their potential fusion with the cell plasma membrane and overcome the impact of LA incorporation on FRET (Fig. 4a), the experiment was designed such that the FRET ratio was calculated from DiO donor emission in DiO&DiI-containing αLA-liposomes, before and following application to cells, relative to DiO emission from DiO-only containing liposomes (Fig. 6). The liposome interactions with A549 cells were quantitatively analysed by both fluorescence spectroscopy readings and flow cytometry (Fig. 6a and b).

Data obtained from fluorescence spectroscopy show that FRET ratios for both αLA$_0$- and αLA$_{20}$-DiO&DiI liposomes following cell exposure are reduced from 0.91 ± 0.02 and 0.85 ± 0.08, to 0.31 ± 0.04 and 0.43 ± 0.05, respectively (Fig. 6a). This reduction in FRET (*i.e.* an increase in donor DiO emission from DiO&DiI-liposomes which would occur on separation of the FRET pair) indicates that changes in the liposomal lipid bilayer structure occurred for both sets of liposomes following their 4-hours incubation with cells. Data from the analysis by flow cytometry corroborate with fluorescence spectroscopy data (Fig. 6b and histogram plots); these also show a decrease in the FRET ratios of both sets of liposomes upon incubation with A549 cells, relative to a control (also in ESI Fig. S5†). Interestingly, the cell population data (Fig. 6c) illustrate a significantly higher association of αLA$_{20}$-containing liposomes with cells, relative to αLA$_0$-liposomes (*e.g.* MFI values for DiO-labelled liposomes of ~142 000 *vs.* 70 000, respectively), which one can consider important from the efficiency in drug delivery perspective.

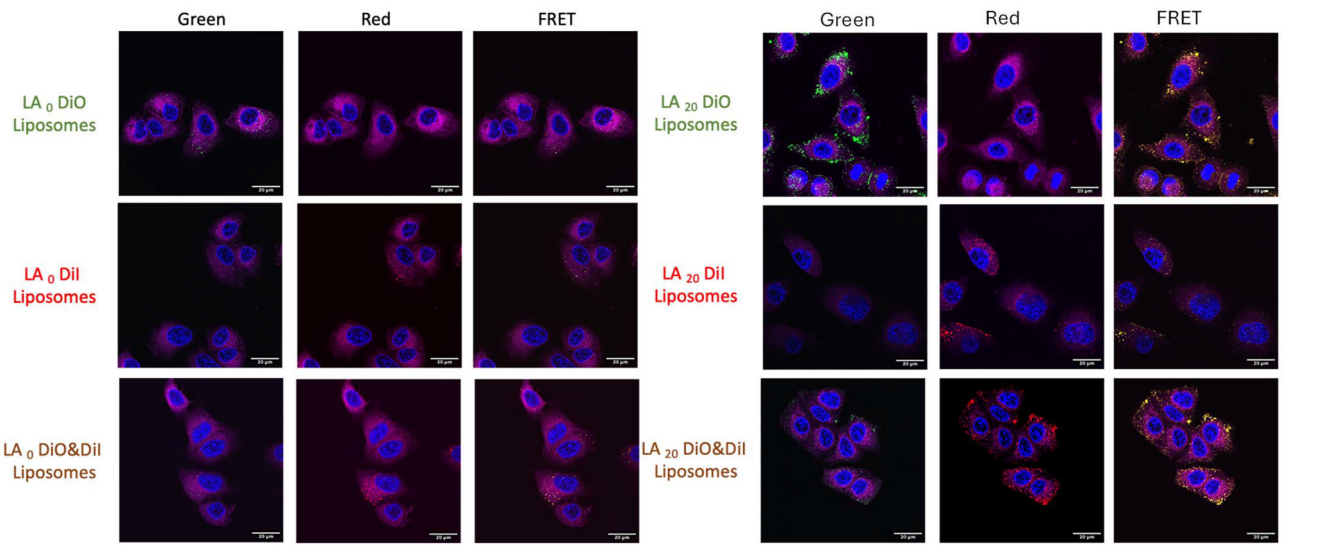

Fig. 7 Confocal fluorescence microscopy images of A549 cells after 4 h of incubation with αLA$_0$-DiO, αLA$_0$-DiI, and αLA$_0$-DiO&DiI and αLA$_{20}$-DiO, αLA$_{20}$-DiI, and αLA$_{20}$-DiO&DiI liposomes at 37 °C. The cells were stained with CellMask™ deep plasma membrane stain (red) and DAPI nuclear stain (blue). Scale bar = 20 μm (63× magnification). The samples were imaged at green (λ_{ex} = 488 nm and λ_{em} = 490–520 nm), red (λ_{ex} = 532 nm and λ_{em} = 545–580 nm), and FRET (λ_{ex} = 488 nm and λ_{em} = 545–580 nm) channels.

Assessment of liposome interactions with cells by confocal laser scanning microscopy

Confocal laser scanning microscopy was employed to visualize interactions between liposomes and cells (Fig. 7). The images demonstrate a 'pebble' morphology of rounded or ovoid shapes of nuclear staining, indicative of healthy epithelial cells[51] (ESI Fig. S2†). Importantly, A549 cells incubated with αLA_{20}-DiO, -DiI, or -DiO&DiI liposomes exhibit significantly higher fluorescence compared to their αLA_0 counterparts, consistent with the flow cytometry data presented in Fig. 6.

Considering the distribution of fluorescence, the images for αLA_0-liposomes show fluorescence throughout the cells and predominantly within the cytosol and perinuclear region of the cells. In contrast, the images of αLA_{20}-liposomes reveal fluorescence primarily localised at the cellular membrane, with some presence in the cytoplasm (as further illustrated in Fig. 8) following 4 hours of incubation. These observations

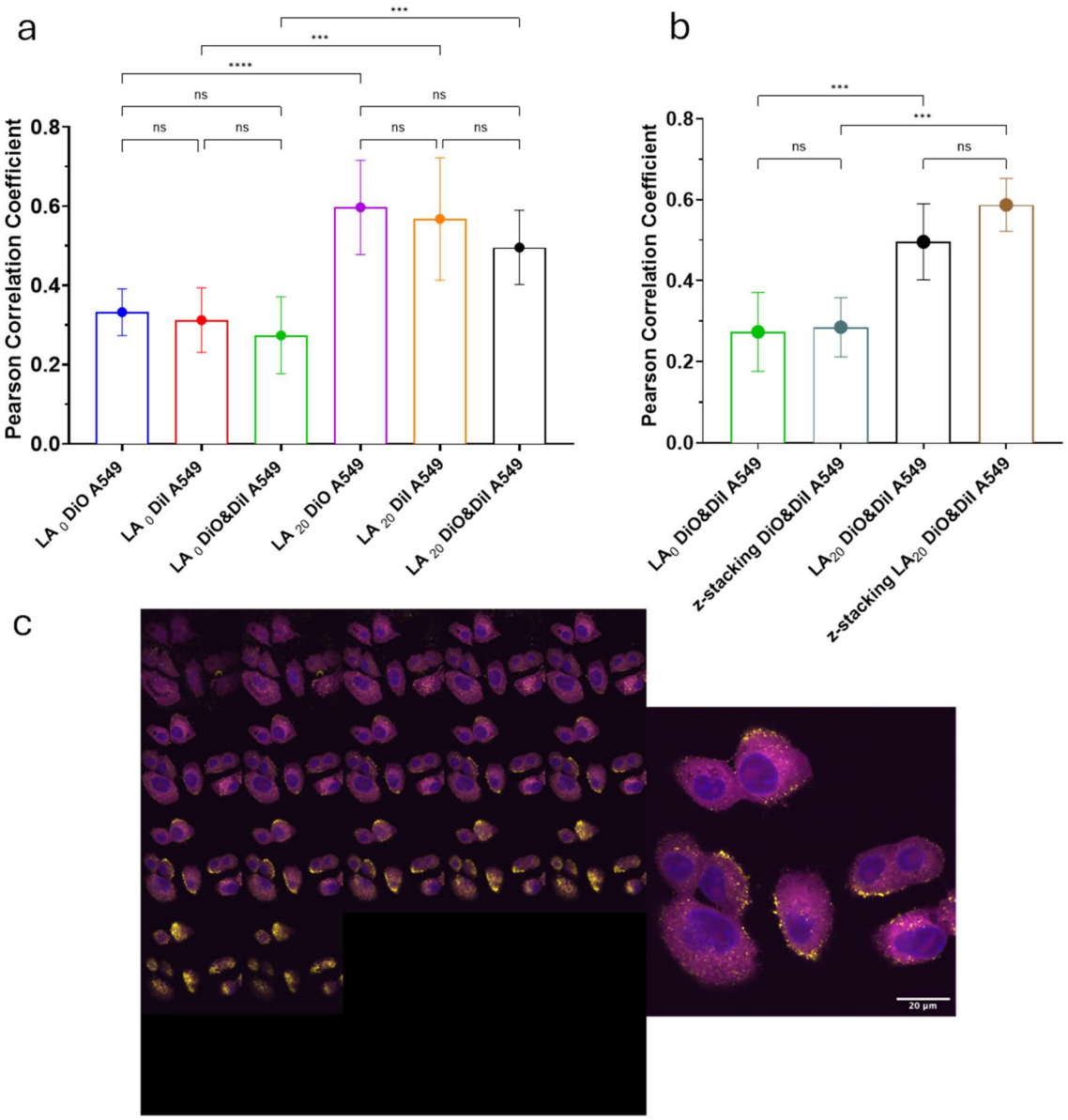

Fig. 8 The Pearson correlation coefficient values for liposomes applied to A549 cells. The coefficient values indicate the degree of colocalization between DiO, DiI, or DiO&DiI fluorescent probes in liposomes and the cell membrane dye, CellMask deep red, as analysed from (a) 2D and (b) the *z*-stacks of images (as illustrated in the confocal image in c). The analysis was performed at a magnification of 40× and 63× using the Jacob plugin in ImageJ software. The experiment was conducted as three replicates (N = 3) with at least two images per replicate (n = >2) whereby the lowest number of cells in one image was 5 cells and a total of >40 cells were analysed. Statistical analysis one-way ANOVA. (c) Confocal fluorescence images of *z*-stack micrographs of A549 cells after 4 h of incubation with 20 mol% αLA-DiO&DiI liposomes at 37 °C. The cells were stained with the CellMask™ deep red plasma membrane and blue DAPI nuclear stain. The samples were imaged at the FRET channel (λ_{ex} = 488 nm and λ_{em} = 545–580 nm). Scale bar = 20 µm (63× magnification).

suggest that αLA_{20}-liposomes preferentially fuse with the plasma membrane rather than undergoing endocytosis. Hence, αLA_0-liposome interactions with cells and subsequent events differ significantly from those of non-αLA-liposomes.

Pearson's correlation coefficient analysis of the confocal microscopy images shown in Fig. 8 includes the coefficient values obtained from both 2D and *z*-stack images (illustrated in Fig. 8) based on pixel intensities for the fluorescent liposomes and cell membrane staining with CellMask. The calculated correlation coefficient values for αLA_0-liposomes are 0.33 ± 0.06, 0.31 ± 0.08, and 0.27 ± 0.10 for DiO, DiI, and DiO&DiI liposomes, respectively. These values indicate a weakly positive correlation,[52–54] suggesting minimal association of fluorescent liposomes and the cell membrane. In contrast, for αLA_{20}-liposomes the correlation values are 0.60 ± 0.12, 0.57 ± 0.15, and 0.50 ± 0.09 for DiO, DiI, and DiO&DiI respectively. These values demonstrate a stronger level of positive correlation, demonstrating a significant correlation in localization of the cell membrane dye and the liposome incorporated dye. This points to a significant role of α-linolenic acid in driving liposome–cell membrane interactions whereby we show that the incorporation of unsaturated α-linolenic acid into the liposomal lipid bilayer increased the membrane fluidity which promotes lipid packing defects.[55] The latter are considered essential for the membrane fusion process to occur.[25]

Importantly, αLA_{20}-Dio&DiI-liposomes exhibit a distinct, heterogeneously distributed pattern of FRET fluorescence puncta located at the A549 cells (Fig. 7). This aligns with a proposed mechanism of membrane fusion which describes merging of lipid membranes as a very site-restricted process that involves defects.[25] For instance, a recent study on interactions of fusogenic liposomes with model membranes (with binary lipid composition and hence the presence of phase separation and defects) shows that, in a regime of low concentration of liposomes, their fusion with the model membrane appears as diffraction-limited dots at specific locations of the model membrane.[56] One should also consider that, importantly for the observations in this study, cholesterol, which is present in the liposomes was used and in the cell plasma membrane, it was shown to mildly reduce the membrane fusion efficiency, but it strongly increases the resilience of membranes against fusion-dependent membrane disruption.[57] Given the mosaic morphology of cell membranes, featuring liquid-disordered (fluid) and liquid-ordered (lipid raft) regions, this pattern might indicate an affinity of αLA – containing liposomes for specific membrane domains.[58,59] The observations here further agree with previous reports, by us and others, regarding the heterogeneous nature of events occurring at the lipid bilayers with complex composition and cell plasma membrane.[60]

Conclusions

This study demonstrates that the incorporation of unsaturated α-linolenic acid (αLA) into the liposomal lipid bilayer, as judged from ^{1}H-NMR spectroscopy, impacts lipid bilayer packing, as indicated by an increase in the fluidity of the liposomal lipid bilayer measured by the laurdan emission assay. The increased fluidity, impact of αLA on the lipid packing, and the presence of lipid domains in the liposomes used here likely create membrane defects and, in this way, promote fusion of αLA liposomes with a simple model-membrane and cell plasma membrane, as indicated by Förster Resonance Energy Transfer (FRET) analysis. Application of confocal microscopy reveals that FRET fluorescence from αLA containing liposomes is preferentially localized at the cell plasma membrane, rather than cellular internalization seen for their non-αLA counterparts, pointing to a preferential liposomal membrane fusion with the plasma membrane. Importantly, the FRET-αLA containing liposomes show a heterogeneously distributed pattern of fluorescence puncta at the cell membrane, even at 4 hours of incubation, suggesting that the fusion is a site-restricted process that might be occurring preferentially at certain membrane domains. These findings are important in providing fundamental understanding in designed drug delivery systems capable of achieving direct cytoplasmic delivery of active compounds, whereby future studies will need to be focused on the selectivity of a fusion location with the cell plasma membrane, the mixing of liposome content with cell cytosol, and such a designed system's potential for drug delivery.

Author contributions

Aljasser: methodology, investigation, and initial draft; Elbahr: methodology and investigation, Bosquillon: supervision and editing, Stolnik: conceptualization, review, editing, supervision, and funding acquisition.

Conflicts of interest

There are no conflicts to declare.

Data availability

The authors state that the supplementary data and the results of this study can be found within the paper and its ESI.† If raw data are required, they can be provided by the corresponding author upon request.

Acknowledgements

AA is grateful to Imam Abdulrahman bin Faisal University, Saudi Arabia, for the funding provided during PhD. AA acknowledges the assistance of Drs Rosa Catania and Nicola Osborne in acquiring NMR data and their analysis. Cryo-TEM work was supported by the Nanoscale and Microscale Research Centre (nmRC) at the University of Nottingham.

References

1 M. J. Hope, M. B. Bally, L. D. Mayer, A. S. Janoff and P. R. Cullis, Generation of multilamellar and unilamellar phospholipid vesicles, *Chem. Phys. Lipids*, 1986, **40**(2–4), 89–107, DOI: 10.1016/0009-3084(86)90065-4.

2 G. Bozzuto and A. Molinari, Liposomes as nanomedical devices, *Int. J. Nanomed.*, 2015, **10**, 975–999, DOI: 10.2147/IJN.S68861.

3 P. C. Lin, S. Lin, P. C. Wang and R. Sridhar, Techniques for physicochemical characterization of nanomaterials, *Biotechnol. Adv.*, 2014, **32**(4), 711–726, DOI: 10.1016/J.BIOTECHADV.2013.11.006.

4 E. B. Manaia, M. P. Abuçafy, B. G. Chiari-Andréo, B. L. Silva, J. A. Oshiro Junior and L. A. Chiavacci, Physicochemical characterization of drug nanocarriers, *Int. J. Nanomed.*, 2017, **12**, 4991–5011, DOI: 10.2147/IJN.S133832.

5 A. C. Apolinário, L. Hauschke, J. R. Nunes and L. B. Lopes, Lipid nanovesicles for biomedical applications: 'What is in a name'?, *Prog. Lipid Res.*, 2021, **82**, 101096, DOI: 10.1016/J.PLIPRES.2021.101096.

6 C. R. Miller, B. Bondurant, S. D. McLean, K. A. McGovern and D. F. O'Brien, Liposome-cell interactions in vitro: Effect of liposome surface charge on the binding and endocytosis of conventional and sterically stabilized liposomes, *Biochemistry*, 1998, **37**(37), 12875–12883, DOI: 10.1021/bi980096y.

7 R. Bajoria, S. R. Sooranna and S. F. Contractor, Endocytotic uptake of small unilamellar liposomes by human trophoblast cells in culture, *Hum. Reprod.*, 1997, **12**(6), 1343–1348, DOI: 10.1093/humrep/12.6.1343.

8 R. M. Straubinger, K. Hong, D. S. Friend and D. Papahadjopoulos, Endocytosis of liposomes and intracellular fate of encapsulated molecules: Encounter with a low pH compartment after internalization in coated vesicles, *Cell*, 1983, **32**(4), 1069–1079, DOI: 10.1016/0092-8674(83)90291-X.

9 D. Papahadjopoulos, G. Poste and B. E. Schaeffer, Fusion of mammalian cells by unilamellar lipid vesicles: Influence of lipid surface charge, fluidity and cholesterol, *Biochim. Biophys. Acta, Biomembr.*, 1973, **323**(1), 23–42, DOI: 10.1016/0005-2736(73)90429-X.

10 V. Torchilin, Intracellular delivery of protein and peptide therapeutics, *Drug Discovery Today Technol.*, 2008, **5**(2–3), e95–e103, DOI: 10.1016/j.ddtec.2009.01.002.

11 W. D. Ehringer, D. Belcher, S. R. Wassall and W. Stillwell, A comparison of α-linolenic acid (18:3ω3) and γ-linolenic acid (18:3ω6) in phosphatidylcholine bilayers, *Chem. Phys. Lipids*, 1991, **57**(1), 87–96, DOI: 10.1016/0009-3084(91)90053-E.

12 J. R. Kanicky and D. O. Shah, Effect of degree, type, and position of unsaturation on the pKa of long-chain fatty acids, *J. Colloid Interface Sci.*, 2002, **256**(1), 201–207, DOI: 10.1006/jcis.2001.8009.

13 S. Leekumjorn, H. J. Cho, Y. Wu, N. T. Wright, A. K. Sum and C. Chan, The role of fatty acid unsaturation in minimizing biophysical changes on the structure and local effects of bilayer membranes, *Biochim. Biophys. Acta, Biomembr.*, 2009, **1788**(7), 1508–1516, DOI: 10.1016/j.bbamem.2009.04.002.

14 K. Arnold, O. Zschoernig, D. Barthel and W. Herold, Exclusion of poly(ethylene glycol) from liposome surfaces, *Biochim. Biophys. Acta, Biomembr.*, 1990, **1022**(3), 303–310, DOI: 10.1016/0005-2736(90)90278-V.

15 B. R. Lentz and J. Lee, Poly(ethylene glycol) (PEG)-mediated fusion between pure lipid bilayers: a mechanism in common with viral fusion and secretory vesicle release? (Review), *Mol. Membr. Biol.*, 1999, **16**(4), 279–296, DOI: 10.1080/096876899294508.

16 W. A. Talbot, L. X. Zheng and B. R. Lentz, Acyl Chain Unsaturation and Vesicle Curvature Alter Outer Leaflet Packing and Promote Poly(ethylene glycol)-Mediated Membrane Fusion, *Biochemistry*, 1997, **36**(19), 5827–5836, DOI: 10.1021/bi962437i.

17 J. Lee and B. R. Lentz, Evolution of Lipidic Structures during Model Membrane Fusion and the Relation of This Process to Cell Membrane Fusion, *Biochemistry*, 1997, **36**(21), 6251–6259, DOI: 10.1021/bi970404c.

18 S. L. Yefimova, I. Y. Kurilchenko, T. N. Tkacheva, *et al.*, Microspectroscopic study of liposome-to-cell interaction revealed by förster resonance energy transfer, *J. Fluoresc.*, 2014, **24**(2), 403–409, DOI: 10.1007/s10895-013-1305-8.

19 ThermoFisher. The Molecular Probes ® Handbook Molecular Probes ™ Handbook for Probes Lipids and Derivatives Membranes Fluorophores. Published online 2010.

20 A. Pitchaimani, T. D. T. Nguyen and S. Aryal, Natural killer cell membrane infused biomimetic liposomes for targeted tumor therapy, *Biomaterials*, 2018, **160**, 124–137, DOI: 10.1016/j.biomaterials.2018.01.018.

21 A. D. Bangham, M. M. Standish and J. C. Watkins, Diffusion of Univalent Ions across the Lamellae of Swollen Phospholipids, *J. Mol. Biol.*, 1965, **13**, 238–252, DOI: 10.1016/S0022-2836(65)80093-6, IN26–IN27.

22 K. W. Dunn, M. M. Kamocka and J. H. McDonald, A practical guide to evaluating colocalization in biological microscopy, *Am. J. Physiol.: Cell Physiol.*, 2011, **300**(4), C723–C742, DOI: 10.1152/ajpcell.00462.2010.

23 C. Hald Albertsen, J. A. Kulkarni, D. Witzigmann, M. Lind, K. Petersson and J. B. Simonsen, The role of lipid components in lipid nanoparticles for vaccines and gene therapy, *Adv. Drug Delivery Rev.*, 2022, **188**, 114416, DOI: 10.1016/j.addr.2022.114416.

24 J. P. Slotte, Sphingomyelin–cholesterol interactions in biological and model membranes, *Chem. Phys. Lipids*, 1999, **102**(1–2), 13–27, DOI: 10.1016/S0009-3084(99)00071-7.

25 G. Cevc and H. Richardsen, Lipid vesicles and membrane fusion, *Adv. Drug Delivery Rev.*, 1999, **38**(3), 207–232, DOI: 10.1016/S0169-409X(99)00030-7.

26 M. Paez-Perez, I. A. Russell, P. Cicuta and L. Di Michele, Modulating membrane fusion through the design of fusogenic DNA circuits and bilayer composition, *Soft Matter*, 2022, **18**(37), 7035–7044, DOI: 10.1039/D2SM00863G.

27 A. Alshehri, A. Grabowska and S. Stolnik, Pathways of cellular internalisation of liposomes delivered siRNA and effects on siRNA engagement with target mRNA and silencing in cancer cells, *Sci. Rep.*, 2018, **8**(1), 3748, DOI: 10.1038/s41598-018-22166-3.

28 L. Degrand, R. Garcia, K. Crouvisier Urion and W. Guiga, Dynamic light scattering for the determination of linoleic acid critical micelle concentration, Effect of pH, ionic strength, and ethanol, *J. Mol. Liq.*, 2023, **388**, 122670, DOI: 10.1016/j.molliq.2023.122670.

29 J. Sabín, G. Prieto, J. M. Ruso, R. Hidalgo-Álvarez and F. Sarmiento, Size and stability of liposomes: A possible role of hydration and osmotic forces, *Eur. Phys. J. E: Soft Matter Biol. Phys.*, 2006, **20**(4), 401–408, DOI: 10.1140/epje/i2006-10029-9.

30 K. Makino, T. Yamada, M. Kimura, T. Oka, H. Ohshima and T. Kondo, Temperature- and ionic strength-induced conformational changes in the lipid head group region of liposomes as suggested by zeta potential data, *Biophys. Chem.*, 1991, **41**(2), 175–183, DOI: 10.1016/0301-4622(91)80017-L.

31 E. Chibowski and A. Szcześ, Zeta potential and surface charge of DPPC and DOPC liposomes in the presence of PLC enzyme, *Adsorption*, 2016, **22**(4–6), 755–765, DOI: 10.1007/s10450-016-9767-z.

32 F. Castelli, S. Caruso and N. Uccella, Biomimesis of Linolenic Acid Transport through Model Lipidic Membranes by Differential Scanning Calorimetry, *J. Agric. Food Chem.*, 2003, **51**(4), 851–855, DOI: 10.1021/jf020582z.

33 T. M. Allen, G. A. Austin, A. Chonn, L. Lin and K. C. Lee, Uptake of liposomes by cultured mouse bone marrow macrophages: influence of liposome composition and size, *Biochim. Biophys. Acta, Biomembr.*, 1991, **1061**(1), 56–64, DOI: 10.1016/0005-2736(91)90268-D.

34 D. Montizaan, K. Yang, C. Reker-Smit and A. Salvati, Comparison of the uptake mechanisms of zwitterionic and negatively charged liposomes by HeLa cells, *Nanomedicine*, 2020, 30, DOI: 10.1016/j.nano.2020.102300.

35 D. S. Wishart, C. Knox, A. C. Guo, *et al.*, HMDB: a knowledgebase for the human metabolome, *Nucleic Acids Res.*, 2009, **37**, D603–D610, DOI: 10.1093/NAR/GKN810.

36 A. S. Klymchenko, S. Oncul, P. Didier, *et al.*, Visualization of lipid domains in giant unilamellar vesicles using an environment-sensitive membrane probe based on 3-hydroxyflavone, *Biochim. Biophys. Acta, Biomembr.*, 2009, **1788**(2), 495–499, DOI: 10.1016/j.bbamem.2008.10.019.

37 E. Sezgin, I. Levental, M. Grzybek, *et al.*, Partitioning, diffusion, and ligand binding of raft lipid analogs in model and cellular plasma membranes, *Biochim. Biophys. Acta, Biomembr.*, 2012, **1818**(7), 1777–1784, DOI: 10.1016/j.bbamem.2012.03.007.

38 S. S. Antollini and M. I. Aveldaño, Thermal behavior of liposomes containing PCs with long and very long chain PUFAs isolated from retinal rod outer segment membranes, *J. Lipid Res.*, 2002, **43**(9), 1440–1449, DOI: 10.1194/JLR.M200057-JLR200.

39 G. Bianchetti, S. Azoulay-Ginsburg, N. Y. Keshet-Levy, *et al.*, Investigation of the Membrane Fluidity Regulation of Fatty Acid Intracellular Distribution by Fluorescence Lifetime Imaging of Novel Polarity Sensitive Fluorescent Derivatives, *Int. J. Mol. Sci.*, 2021, **22**(6), 3106, DOI: 10.3390/ijms22063106.

40 C. S. Poojari, K. C. Scherer and J. S. Hub, Free energies of membrane stalk formation from a lipidomics perspective, *Nat. Commun.*, 2021, **12**(1), 6594, DOI: 10.1038/s41467-021-26924-2.

41 A. Sharma and U. S. Sharma, Liposomes in drug delivery: Progress and limitations, *Int. J. Pharm.*, 1997, **154**(2), 123–140, DOI: 10.1016/S0378-5173(97)00135-X.

42 A. Akbarzadeh, R. Rezaei-Sadabady, S. Davaran, *et al.*, Liposome: Classification, preparation, and applications, *Nanoscale Res. Lett.*, 2013, **8**(1), 1–9, DOI: 10.1186/1556-276X-8-102/TABLES/2.

43 M. B. Lande, J. M. Donovan and M. L. Zeidel, The relationship between membrane fluidity and permeabilities to water, solutes, ammonia, and protons, *J. Gen. Physiol.*, 1995, **106**(1), 67–84, DOI: 10.1085/JGP.106.1.67.

44 G. W. Feigenson, Phase behavior of lipid mixtures, *Nat. Chem. Biol.*, 2006, **2**(11), 560–563, DOI: 10.1038/nchembio1106-560.

45 S. L. Veatch, I. V. Polozov, K. Gawrisch and S. L. Keller, Liquid Domains in Vesicles Investigated by NMR and Fluorescence Microscopy, *Biophys. J.*, 2004, **86**(5), 2910–2922, DOI: 10.1016/S0006-3495(04)74342-8.

46 X. Zhao, X. Ma, J. H. Dupius, *et al.*, Negatively charged phospholipids accelerate the membrane fusion activity of the plant-specific insert domain of an aspartic protease, *J. Biol. Chem.*, 2022, **298**(1), 101430, DOI: 10.1016/j.jbc.2021.101430.

47 J. M. Hernandez, A. Stein, E. Behrmann, *et al.*, Membrane Fusion Intermediates via Directional and Full Assembly of the SNARE Complex, *Science*, 2012, **336**(6088), 1581, DOI: 10.1126/SCIENCE.1221976.

48 A. P. Wong and J. T. Groves, Molecular topography imaging by intermembrane fluorescence resonance energy transfer, *Proc. Natl. Acad. Sci. U. S. A.*, 2002, **99**(22), 14147–14152, DOI: 10.1073/PNAS.212392599.

49 C. Ghatak, V. G. Rao, R. Pramanik, S. Sarkar and N. Sarkar, The effect of membrane fluidity on FRET parameters: an energy transfer study inside small unilamellar vesicle, *Phys. Chem. Chem. Phys.*, 2011, **13**(9), 3711–3720, DOI: 10.1039/C0CP01925A.

50 Q. Lubart, J. K. Hannestad, H. Pace, *et al.*, Lipid vesicle composition influences the incorporation and fluorescence properties of the lipophilic sulphonated carbocyanine dye SP-DiO, *Phys. Chem. Chem. Phys.*, 2020, **22**(16), 8781–8790, DOI: 10.1039/C9CP04158C.

51 E. G. Fischer, Nuclear Morphology and the Biology of Cancer Cells, *Acta Cytol.*, 2020, **64**(6), 511–519, DOI: 10.1159/000508780.

52 D. Ratnasari, F. Nazir, L. O. H. Z. Toresano, S. A. Pawiro and D. S. Soejoko, The correlation between effective renal

plasma flow (ERPF) and glomerular filtration rate (GFR) with renal scintigraphy 99mTc-DTPA study, *J. Phys.: Conf. Ser.*, 2016, **694**, 012062, DOI: **10.1088/1742-6596/694/1/012062**.

53 T. S. Wahyuni and K. K. Purwanto, Students' conceptual understanding on acid-base titration and its relationship with drawing skills on a titration curve, *J. Phys.: Conf. Ser.*, 2020, **1440**, 012018, DOI: **10.1088/1742-6596/1440/1/012018**.

54 M. M. Mukaka, Statistics corner: A guide to appropriate use of correlation coefficient in medical research, *Malawi Med. J.l*, 2012, **24**(3), 69–71.

55 J. Bigay and B. Antonny, Curvature, Lipid Packing, and Electrostatics of Membrane Organelles: Defining Cellular Territories in Determining Specificity, *Dev. Cell*, 2012, **23**(5), 886–895, DOI: **10.1016/j.devcel.2012.10.009**.

56 R. R. M. Cavalcanti, R. B. Lira, E. J. Ewins, R. Dimova and K. A. Riske, Efficient liposome fusion to phase-separated giant vesicles, *Biophys. J.*, 2023, **122**(11), 2099–2111, DOI: **10.1016/j.bpj.2022.12.008**.

57 R. B. Lira, J. C. F. Hammond, R. R. M. Cavalcanti, M. Rous, K. A. Riske and W. H. Roos, The underlying mechanical properties of membranes tune their ability to fuse, *J. Biol. Chem.*, 2023, **299**(12), 105430, DOI: **10.1016/j.jbc.2023.105430**.

58 S. Munro, Lipid Rafts: Elusive or Illusive?, *Cell*, 2003, **115**(4), 377–388, DOI: **10.1016/S0092-8674(03)00882-1**.

59 A. S. Shaw, Lipid rafts: Now you see them, now you don't, *Nat. Immunol.*, 2006, **7**(11), 1139–1142, DOI: **10.1038/ni1405**.

60 R. Cavanagh, S. Shubber, D. Vllasaliu and S. Stolnik, Enhanced permeation by amphiphilic surfactant is spatially heterogenous at membrane and cell level, *J. Controlled Release*, 2022, **345**, 734–743, DOI: **10.1016/j.jconrel.2022.03.053**.